Journal Pre-proof

An integrated fluorescence biosensor for microRNA detection based on exponential amplification reaction-triggered three-dimensional bipedal DNA walkers

Liu Yang, Jie Fang, Junjie Li, Xinying Ou, Li Zhang, Yufeng Wang, Zhi Weng, Guoming Xie

PII: S0003-2670(20)31173-9

DOI: https://doi.org/10.1016/j.aca.2020.11.043

Reference: ACA 238111

To appear in: *Analytica Chimica Acta*

Received Date: 1 October 2020

Revised Date: 23 November 2020

Accepted Date: 27 November 2020

Please cite this article as: L. Yang, J. Fang, J. Li, X. Ou, L. Zhang, Y. Wang, Z. Weng, G. Xie, An integrated fluorescence biosensor for microRNA detection based on exponential amplification reaction-triggered three-dimensional bipedal DNA walkers, *Analytica Chimica Acta*, https://doi.org/10.1016/j.aca.2020.11.043.

Credit Author Statement

The contribution of each author to this work as following:

Liu Yang: Design of this work, performing the experiments and writing.

Jie Fang: Design of this work.

Junjie Li: Design of this work and reviewing.

Xinying Ou: Reviewing and editing.

Li Zhang: Drawing.

Yufeng Wang: Data collection.

Zhi Weng: Data collection.

Guoming Xie: Reviewing and editing, supervision and funding acquisition.

Graphical abstract

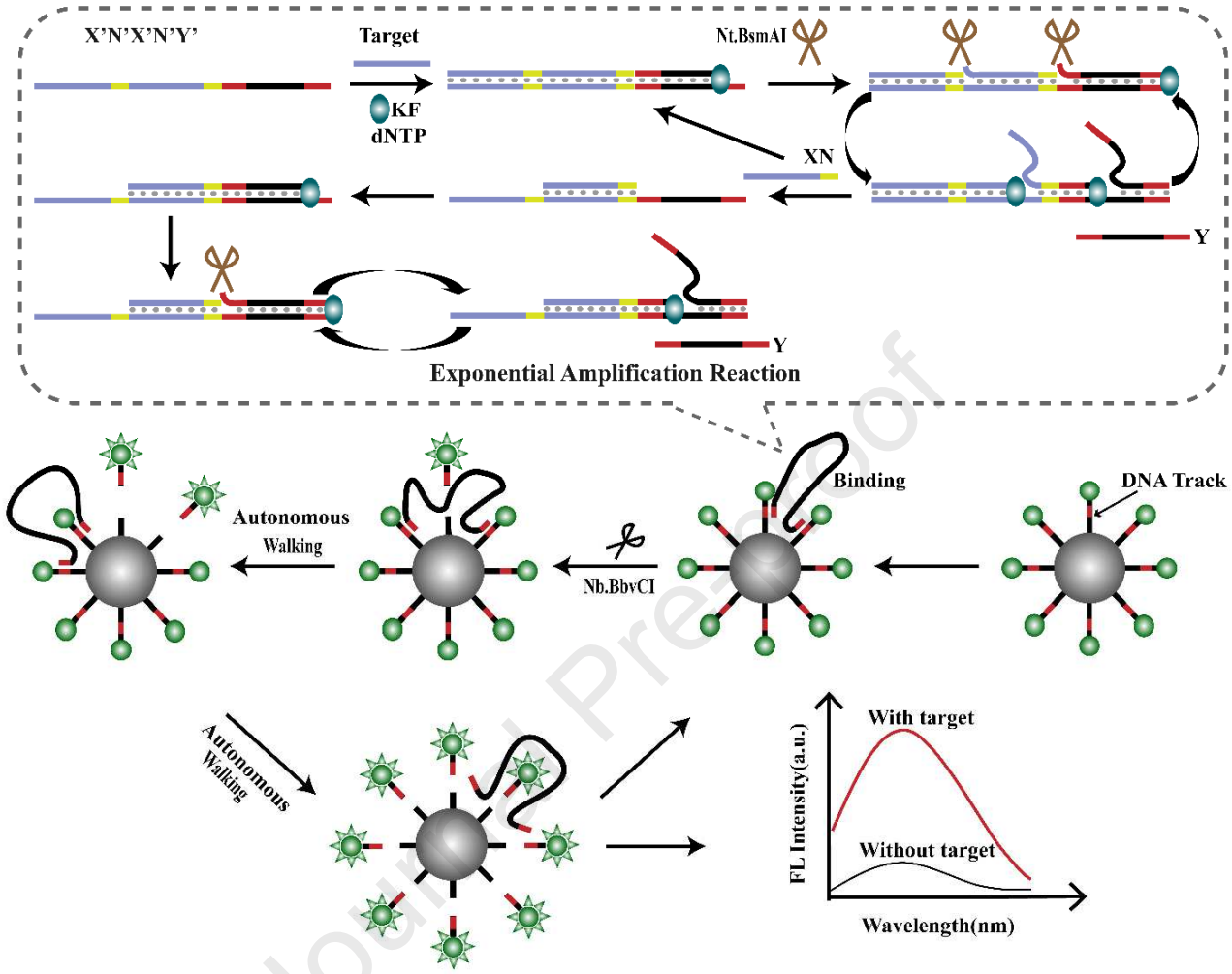

EXPAR-BDW strategy based on exponential amplification reaction-triggered three-dimensional bipedal DNA walkers.

An integrated fluorescence biosensor for microRNA detection based on exponential amplification reaction-triggered three-dimensional bipedal DNA walkers

Liu Yang, Jie Fang, Junjie Li, Xinying Ou, Li Zhang, Yufeng Wang, Zhi Weng, and Guoming Xie*

Key Laboratory of Laboratory Medical Diagnostics of Education, Ministry of Education, Department of Laboratory Medicine, Chongqing Medical University, Chongqing 400016, PR China

*Correspondence author: Tel: +86 23 68485240; Fax: +86 23 68485239

E-mail address: guomingxie@cqmu.edu.cn and xiegm059@foxmail.com

Abstract

Sensitive and specific miRNA detection is essential for the early cancer diagnosis. In this work, we design a fluorescent microRNA biosensor based on exponential amplification reaction (EXPAR) and nicking endonuclease-powered three-dimensional (3-D) bipedal DNA walkers (BDW). Target microRNA initiates EXPAR with the help of polymerase and nicking endonuclease to generate the large number of BDW in solution. The newly generated BDW can be continuously assembled onto polystyrene microsphere track co-modified with fluorescence-labelled DNA strand. Thus, in the presence of nicking endonuclease, the walking machine is activated to produce enhanced fluorescent signal in the supernatant. Besides, we prove that BDW holds the faster walking speed than single-legged DNA walker (SDW) based on comparative study. Under optimal conditions, the proposed amplification method owns a wide linear range from 10 fM to 5 nM with a detection limit down to 5.2 fM. The reaction time of the assay takes about 70 min. The combination of enzyme-assisted EXPAR in solution and enzyme-powered BDW on particle significantly increases the signal amplification efficiency and improves the detection sensitivity. Therefore, our method has enormous potential for the application of BDW-related biosensors.

Keywords: Exponential amplification reaction; DNA walker; Enzymatic amplification; Fluorescence biosensor; Nucleic acid detection

1. Introduction

DNA walker, as one of DNA nanomachines, has aroused tremendous attention due to its exceptional properties of automaticity and controllability [1]. For example, Tan et al presented a photon-fueled DNA walker capable of regulating autonomous movement along a nucleic acid track [2]. Tinnefeld's group proposed a DNA walker that strode on a DNA origami track based on fluorescence signal amplifier [3]. Nevertheless, both one-dimensional (1-D) footpath and two-dimensional (2-D) DNA origami have very limited processivity and confined travel space, which constrain the executive ability of such DNA walking nanomachines [2-4]. To settle above problems, researchers recently established 3-D tracks on the surface of microspheres or nanoparticles [5-8]. Because of the increased local e□ective concentrations, thus perform enhanced walking steps and high processivity compared to the 1-D and 2-D tracks. In the meantime, much efforts have also been devoted to exploring multiple styles of drive motor of DNA walkers. The driving forces for most are provided by toehold–mediated strand displacement and DNAzyme/endonuclease/exonuclease–mediated hydrolysis [9-13]. Among them, the adoption of highly active nucleic acid tool enzymes presents superior ability due to accelerated walking speed [14]. This is on one hand attributed to the enzyme's natural high catalytic capacity. On the other hand, owing to intraparticle interactions and increased local substrate concentrations, biocatalysis on particles can accelerate enzymatic reactions [15]. For instance, Li's group introduced a nicking endonuclease-powered stochastic 3-D DNA walker that

moves rapidly on a 20 nm gold nanoparticle. Such 3-D DNA walker demonstrated remarkably high processivity and fast mass transfer [16]. More importantly, this type of DNA walker has been widely used recently [17, 18].

It is worth noting that the DNA walkers mentioned above hold one swing arm assembled on the surface of nanoparticles, which restricts the movement scope and efficiency of DNA walking machines. In addition, the construction of two different probes on the same microsphere or nanoparticle surface may not only diminish the local concentration of track DNA as a consequence of the occupation of the swing arm but also increase the difficulty of fabricating multiple DNA probes with different concentration ratios [19]. To address this issue, a few bipedal DNA walker strategies were proposed to improve walking efficiency [20, 21]. One of the examples is Li's group, who developed a bottom-up approach to assemble a bipedal DNA walker capable of probing and controlling dynamic interactions at bio-nano interfaces on AuNPs. This method has successfully provided the improved understanding to rationalize the design of enzyme-powered bipedal DNA walker for nucleic acids and proteins biosensors [22].

Apart from on-particle biocatalysis, the construction of a powerful biorecognition component is of equal importance for a 3-D DNA walker. It has been reported that in-solution biorecognition may be better fabricated, predicted, controlled and performed comparing to on-particle biorecognition [15]. On the other hand, the routine analysis of a target molecule yields only one DNA walker, thus limiting the total number of DNA walkers and their walking efficiency [23]. Therefore, a method

that integrates biorecognition and amplification in solution is desirable. Recently, isothermal amplification strategies have emerged as powerful tools for the analysis of nucleic acids, proteins and other molecules [24-26] . Among them, exponential amplification reaction (EXPAR), on account of the outstanding advantages of high amplification efficiency (10^6-10^8) and simple operation, has gained attention in the design of sensitive sensors [27-31]. Induced by polymerase and nicking endonuclease, EXPAR amplifies a large amount of single-stranded DNA (ssDNA) with the activation of specific primers in a short time (<30 min) [32]. Therefore, enzyme-powered bipedal 3-D DNA walker coupled with enzyme-assisted EXPAR in analysis of low-abundance biomolecules is significant.

In this work, a new 3-D DNA walker sensor was constructed integrated EXPAR in solution with enzymatic cleavage reaction on microparticle for highly sensitive and selective detection of microRNA. MicroRNA 21 is used as a model target because it plays a crucial role in a plethora of biological functions and diseases including development, cancer, cardiovascular diseases and inflammation [33]. Our system includes two reaction circuits in series. EXPAR as the first reaction is triggered upon introduction of the target microRNA together with the releasement of massive ssDNA strands. An ssDNA strand functions as a BDW and then is continuously assembled onto DNA-modified polystyrene microsphere surface. The second reaction is an enzyme-powered 3-D DNA walker which is activated by nicking endonuclease to perform roboticized and stepwise movements around the DNA tracks, causing the persistent fluorescence signals output. The two reaction circuits ensure high

sensitivity of the developed method, providing a potential platform for microRNA analysis and a powerful tool for nucleic acid detection.

2. Experimental part

2.1 Materials and reagents

All the DNA and RNA sequences used in this study were synthesized by Sangon Biotech Inc. (Shanghai, China) with HPLC purification and their detail base sequences were listed in Table S1 respectively. Klenow fragment polymerase (KF, 3'→ 5' exo-), Nt.BsmAI NEase, Nb.BbvCI NEase, 10 × CutSmart buffer (20 mM Tris-acetate, 50 mM potassium acetate, 10 mM magnesium acetate and 100 μg/ml BSA, pH 7.9) and 10 × NEBuffer 2 (50 mM NaCl ,10 mM Tris–HCl, 10 mM $MgCl_2$, and 1 mM dithiothreitol, pH 7.9) were purchased from New England Biolabs (USA). Streptavidin-coated polystyrene microspheres were obtained from Spherotech (GER). 20 bp DNA Ladder, 6 × DNA loading buffer and Gel Red nucleic acid dye were provided by TaKaRa Biotech (Dalian, China). Ammonium persulfate (APS), N,N,N′,N′-tetramethylethylenediamine (TEMED), 30% acrylamide/bis solution , deoxynucleotide triphosphates (dNTPs), diethylpyrocarbonate (DEPC)-treated water and TE buffer (10 mmol/L Tris-HCl,1 mmol/L EDTA, pH 8) were ordered from Sangon Biotech Inc. (Shanghai, China). Binding buffer (20 mM Tris-HCl, 1 M NaCl, 1 mM EDTA, 0.0005% Triton X-100, pH 7.5) was prepared in our laboratory. All other chemicals were of reagent grade and used without any further purification.

2.2 Apparatus

Fluorescence signals were measured on a Cary Eclipse Fluorescence Spectrophotometer (Agilent, California), using a quartz fluorescence cuvette with an optical path length of 1.0 cm. The excitation wavelength was set at 480 nm with emission spectra range of 500-600 nm. The excitation and emission slit widths were made at 5 nm and 10 nm, respectively. EXPAR was monitored by CFX96^{TM} Real-Time PCR detection system (Bio-Rad, USA). The non-denaturing polyacrylamide gel electrophoresis (PAGE) was carried out on DYY-6C electrophoresis (DYY6C, LiuYi, China) and the gel was imaged on a Bio-Rad ChemDoc XRS (Bio-Rad, USA).

2.3 Isothermal exponential amplification reaction (EXPAR)

First of all, 100 nM template, various concentrations of target microRNA, 1 μL 10×CutSmart buffer and 1 μL 10×NEBuffer 2 were mixed and heated to 95 °C for 5 min in the water bath, followed by slowly decreasing to room temperature. Then, 0.2 U of KF polymerase, 1U of Nt.BsmAI, 250 μM dNTP and DEPC-treated water were added to the mixture in a final volume of 10 μL. The amplification reaction was conducted at 37 °C for 30 min. Finally, the reaction system was terminated by enzyme inactivation treatment at 80 °C for 20 min. The solution was stored at 4 °C for further use. The experiments above were repeated three times to reduce experimental error.

2.4 Preparation of the DNA walker probes

The 50 μL of streptavidin-coated microspheres were washed twice with 50 μL binding buffer by centrifuging the microspheres at 12000 rpm for 3 min and discarding the supernatant. After resuspending with 50 μL binding buffer, 5 μL of 20

μM track strands were added into the microspheres. The track strands were modified with biotin at 5' terminus and labeled with fluorescent dye carboxyfluorescein (FAM) at 3' terminus. The mixture was incubated for 20 min at 37 °C. The above solution was then subjected to centrifugation at 12000 rpm for 3 min. After removing the supernatant, the remaining solution was washed three times with 50 μL TE buffer. Finally, the microsphere complex was suspended with 50 μL TE buffer.

2.5 Fluorescence measurement of microRNA

For a typical walker operation, the reaction solution was performed at 37 °C for 20 min in a 100 μL reaction volume, including 10 μL EXPAR products, 5 μL prepared microsphere complex, 10 U Nb.BbvCI NEase in 1 × CutSmart buffer. After centrifugation of the reaction solution at 12000 rpm for 3 min, the supernatant was collected to measure fluorescence signals. In the reproducibility experiments, the volume was the same as that used in the detection procedure. We only added the number of independent experiments to five.

2.6 Real-Time PCR detection system to monitor EXPAR

The reaction solutions for EXPAR were prepared on ice before being placed in the Real-Time PCR detection system. The EXPAR was carried out in a volume of 10 μL containing 100 nM template, various concentrations of target microRNA, 1 μL 10×CutSmart buffer, 1 μL 10×NEBuffer 2, 250 μM dNTP, 0.2 U of KF polymerase, 1U of Nt.BsmAI, 1 × SYBR-Green and DEPC-treated water. The mixture was incubated at 37 °C and the real-time fluorescence intensity was monitored at intervals of 30s.

2.7 Fluorescence microscope for imaging the walker reaction on microsphere surface

Images of the fluorescent microspheres were acquired by a fluorescence microscope (Nikon 80i, Japan) with 100× objective lens. The prepared microsphere complex that reacted with and without the target was incubated at 37 °C for 20 min followed by washing with TE-Mg^{2+} buffer. 5μL of the prepared microsphere complex and above resulting microspheres were firstly spread on a slide (25 mm×75 mm) and another coverslip (24 mm×50 mm) was put onto the first one. A thin layer of immersion oil was placed between the slip and the objective lens. All of the fluorescence images were collected with 100 ms exposure time by using the NIS-Viewer software.

2.8 Gel electrophoresis

PAGE was carried out on DYY-6C electrophoresis analyzer with 12% native polyacrylamide gel in 0.5×TBE buffer (90 mM Tris-HCl, 90 mM boric acid, 2 mM EDTA, pH 7.9) at 100 V constant voltages for 60 min. For a typical sample analysis, 1 μL of reaction products was mixed with 5 μL 6 × loading buffer and then loaded into the gel. After that, the gel was stained with Gel Red at room temperature for 20 min and imaged.

2.9 LOD calculation

The limit of detection (LOD) is the lowest concentration of an analyte that an analytical process can reliably detect. LOD in our work was defined as LOD=3σ/s,

where σ was the standard deviation of the blank (control samples) and s was the analytical sensitivity, which could be estimated as the slope of calibration plot.

3. Result and discussion

3.1 Principle of the proposed method

The working principle of the assay for microRNA detection based on EXPAR triggered 3-D BDW strategy is illustrated in Scheme 1. The EXPAR template is designed as X'N'X'N'Y'. X' is target microRNA recognition site. Y' is complementary to the sequence of BDW and N' contains a complementary site for Nt.BsmAI nicking. In the presence of target, the template can combine with it and initiate a polymerization reaction along the microRNA 3′-end with the help of KF polymerase and dNTPs. Thus, a double-stranded DNA (dsDNA) containing two recognition sites (5'-GTCTC-3') for the nicking enzyme Nt.BsmAI is produced. Such nicking enzyme cleaves one strand of dsDNA at the next base downstream of the recognition site to obtain amounts of XN and Y repeatedly. At the same time, the newly synthesized XN oligomer which contains the target sequence will hybridize with the template and trigger another cycle reaction. In consequence, the whole reaction brings about an isothermal exponential amplification, producing massive Y strands (BDW). The BDW is designed to have 7 nt complementary nicking cleavage sequence of nicking endonuclease Nb.BbvCI at both 5' and 3' terminus. The substrate track strand is designed to have a 7 nt recognition sequence for Nb.BbvCI nicking whose 5' end is modified with a biotin to tether on the streptavidin-coated microsphere surface and 3'end is labeled with FAM. Thus, BDW can attach to the

track strand on the microsphere surface. With the assistance of Nb.BbvCI, BDW catalyzes the cleavage of track strand at recognition site, resulting in the release of BDW and fluorescence signal. Then, the released BDW hybridizes with another adjacent track strand on the same microsphere. The newly formed DNA duplex can trigger a recycle cleavage process until all track strands are exhausted. Eventually, countless short DNA fragments labeled with FAM will disperse into the solution. After centrifugation and separation, fluorescence signal in the supernatant is recorded by the fluorescence spectrophotometer and the signal intensity is related to the concentration of target microRNA.

<Scheme 1.>

3.2 Feasibility of the EXPAR-BDW reaction

We first clarified EXPAR process using Real-Time PCR detection system. The time-dependent increase in the fluorescence intensity of different target concentrations in the mixture was monitored for 40 min (Fig. 1A). Notably, a significant increase in fluorescence signal was observed for all mixtures in the presence of target (10 fM, 100 fM, 10 pM, 500 pM and 5 nM). In sharp contrast, mixture without target showed a negligible increase in the fluorescence intensity. These findings strongly indicated that the reaction of EXPAR was successful. Furthermore, the EXPAR products were characterized by native polyacrylamide gel electrophoresis (PAGE) to verify the performance of EXPAR. The results were shown in Figure S1.

Then, to confirm the feasibility of enzymatic cleavage reaction of BDW, we

measured the fluorescence signal using 5 nM of BDW in the presence of Nb.BbvCI. A control experiment without BDW was also conducted. As illustrated in Fig. 1B, curve b was the fluorescence response when BDW was no existence. It was seen obviously that weak fluorescence signal was found. While a distinct fluorescence signal increase can be observed in the presence of BDW in curve a. The results manifested the enzymatic cleavage reaction of BDW took place on the microsphere surface. Furthermore, we evaluated the walking behavior of two types of DNA walkers. Single-legged DNA walker (SDW) and BDW with same concentration of track strand were prepared (Fig. 1C). The fluorescence signals of SDW and BDW (5 nM, respectively) at different assay times were shown in Fig. 1D. Notably, the fluorescence intensity of SDW increased at a relatively slow rate until 35 min with a plateau. In comparison, the fluorescence intensity of BDW almost reached a plateau in 20 min. According to the experiment results of Fig. 1D, the initial rate of BDW was calculated to be 16.63 min^{-1} but the initial rate of SDW was only 9.45 min^{-1}. The initial rate of BDW was 1.76-fold higher than that of SDW. However, as the incubation time prolonged, they reached the same value of fluorescence signal. This obviously demonstrated that for SDW and BDW, there was almost no difference in the final response but the walking speed of BDW was faster than SDW.

<Fig. 1.>

To further validate the feasibility of 3-D DNA walker integrated with EXPAR strategy, we tested the fluorescence signals under different conditions. As seen in Fig. 2A, curve a and curve b were the fluorescence responses without KF polymerase or

Nt.BsmAI, respectively. It was clear that almost no fluorescence signal was observed because EXPAR reaction could not be initiated in the absence of polymerase or nicking endonuclease. Curve c was the fluorescence response without Nb.BbvCI. Similarly, still no fluorescent signal was detected. Although EXPAR was initiated, 3-D DNA walker could not be activated in the absence of Nb.BbvCI. Correspondingly, there was almost no fluorescence signal. When target was not added, weak background signal was observed (Curve d). However, a strong fluorescence signal was detected when all reaction elements were added (Curve e). These results demonstrated that each enzyme played an essential role in amplification process, confirming the successful design of two reaction circuits for microRNA detection.

Moreover, to visually confirm that the walker sensor was activated by the target, a fluorescence microscope was also used to validate the feasibility of the walker sensor. As expected, since fluorescence-labelled DNA track strands were successfully modified on microsphere surface, a large number of green fluorescence microspheres were randomly distributed in the field of sight (Fig. 2B). For Fig. 2C, the same green fluorescence was observed when no target was incubated in the reaction system. However, after walker was activated by adding target DNA, few green fluorescence was observed (Fig. 2D), indicating that the EXPAR-triggered DNA walker sensor was completely feasible.

<Fig. 2.>

3.3 Optimization of experimental conditions

To obtain the most efficiency analytical performance of the proposed assay, the EXPAR reaction time, the Nb.BbvCI mediated DNA walker reaction time, the concentration of KF polymerase and the concentration of Nb.BbvCI were optimized.

The exponential nature of the EXPAR renders it prone to nonspecific amplification. These spurious amplifications are always observed with a short delay after the target-triggered reaction [34]. As shown in Fig. 3A, the fluorescence signal intensity increased significantly with the EXPAR reaction time and the signal to background signal ratio (S/B) did not reach a plateau, but reached its maximal value at 30 min. While its value instead dropped after 30 min, since the background signal was also enhanced significantly with the extended reaction time. Hence, the optimum reaction time of EXPAR in this experiment is 30 min. Subsequently, we optimized Nb.BbvCI mediated DNA walker reaction time. As shown in Fig. 3B, it was found that S/B ratio reached maximum in 20 min, suggesting that enzymatic BDW has a rapid walking speed. In addition, enzyme dosage directly affect the efficiency of the reaction and signal output, the concentration of KF polymerase and Nb.BbvCI were optimized to achieve the best analysis results. Fig. 3C presented fluorescence intensity at different KF polymerase concentrations. It was found 0.20 U/10 μL was the optimal concentration. As Nb.BbvCI was another critical element of the walker sensor, we varied concentration of Nb.BbvCI from 1 U/100 μL to 20 U/100 μL. As displayed in Fig. 3D, the fluorescence signal of the walker sensor rose markedly as the concentration of the nicking endonuclease increased, exhibiting the highest

fluorescence intensity at 10 U/100 μL. However, if the concentration of Nb. BbvCI was larger than 10 U/100 μL, the fluorescence intensity would drop slightly. So, the optimal concentration of Nb. BbvCI was adopted as 10 U/100 μL.

<Fig. 3.>

3.4 Analytical performance of the biosensor

Under optimized conditions, we further used different concentrations of microRNA to investigate the sensitivity of the present platform. As illustrated in Fig. 4A, the fluorescence signal increased with increasing the concentration of target microRNA from 10 fM to 5 nM. Furthermore, according to Fig. 4B, the fluorescence intensity exhibited a good linear relationship with the logarithm of target microRNA concentration. The linear regression equation is F=127.231+32.543lgC with a correlation coefficient R^2 of 0.983, where F is the fluorescence intensity and C is the concentration of microRNA 21 (pM). The detection limit is calculated to be 5.2 fM based on the 3σ rule, which is comparable with other reported methods [28, 35, 36]. Strand displacement amplification (SDA) is another isothermal amplification technique with similar principle relying on polymerase and nicking endonuclease [37]. We compared the detection performance of this method with SDA-triggered DNA walker in Figure S4. The detection limit of SDA-triggered DNA walker is only 6.8 pM, which demonstrates that EXPAR-triggered DNA walker possesses a higher detection sensitivity. This superior performance should be attributed to the competing amplification efficiency of EXPAR. Besides, the proposed method was compared with other current methods, indicating a good assay performance of this approach. (Table

S3).

<Fig. 4.>

3.5 Selectivity and reproducibility assay

To evaluate the selectivity of our method, four different control targets with high sequence homology were tested as interference substances, including microRNA 141, microRNA 155, microRNA 199a and let 7a. $(F- F_0)/ F_0$ was compared under identical experimental conditions, where F is the fluorescence intensity for different microRNAs and F_0 is the blank signal. As displayed in Fig. 5A, there were significant differences between target microRNA and other interfering microRNAs. The presence of target microRNA 21 showed a relatively high $(F- F_0)/ F_0$ value compared with other analogs. These results indicated that this proposed method has a good selectivity for distinguishing microRNA 21 from homologues. To assess the reproducibility of the proposed fluorescence biosensor, unequal concentrations of microRNA 21 at 0.01 pM, 10 pM and 500 pM were carried out five times. As shown in Fig. 5B, the relative standard deviations (RSD) were 4.89%, 4.35% and 3.00%, respectively. These results showed that our amplification strategy has satisfactory stability and reliability.

<Fig. 5.>

3.6 Real-sample analysis

The serum is a realistically complex matrix containing a variety of proteins and other contaminants. In order to assess the applicability of the developed biosensor in complex biological samples, we spiked different concentrations of microRNA 21 (0.1 pM, 10 pM and 100 pM) into 10-fold diluted human serum samples (DEPC-treated

water) to mimic the identical environment with real samples, since the capability of this assay to directly detect miRNA in serum will be inhibited by highly complex serum matrix [38, 39]. As seen in Figure 6, responses obtained at 480 nm from the diluted serum practically showed no change compared with buffer. These results indicated that serum does not interfere with the potential analysis capability of our proposed walker sensor.

<Fig. 6.>

4. Conclusions

In summary, we have successfully constructed a three-dimensional bipedal DNA walker through target-triggered EXPAR reaction and applied it to detect microRNA. The dual reaction circuits are achieved via polymerase and endonuclease mediated EXPAR reaction as well as enzyme-driven 3-D DNA walker on polystyrene microspheres. As-proposed dual-amplification of fluorescence signal realizes relatively high sensitivity towards down to 5.2 fM target microRNA. The reaction time of the entire process takes about 70 min, which is faster than most reported multilayer amplification systems. Besides, we evaluated the walking behavior of SDW and BDW. Compared with SDW, the BDW owns a faster walking speed and the initial rate of BDW is 1.76-fold higher than that of SDW. Notably, the whole system only needs to prepare two different nucleic acid strands, one template strand and another substrate strand. Compared with current other isothermal amplification approaches, such as catalytic hairpin self-assembly (CHA) [40], entropy driven

reaction (EDC) [24] and hybridization chain reaction(HCR) [41] , the EXAPR strategy in combination with 3-D DNA walker we adopted in this work avoids complicated nucleic acid design and the possibility of signal leakage owing to multiple nucleic acid strands [42]. Although the involvement of multiple enzymes in the reaction system may make the walker vulnerable to interference in the external circumstances, the proposed method would still provide new strategy for the development of sensitive, simple and rapid fluorescence biosensor.

Acknowledgments

This study was financially supported by the National Natural Science Foundation of China (No. 81672112, 81972025), Chongqing Technology Innovation and Application Demonstration Project (cstc2018jscx-msybX0010).

References

[1] J. Chen, Z. Luo, C. Sun, Z. Huang, C. Zhou, S. Yin, Y. Duan, Y. Li, Research progress of DNA walker and its recent applications in biosensor, TrAC Trends in Analytical Chemistry 120 (2019) 115626.

[2] M. You, Y. Chen, X. Zhang, H. Liu, R. Wang, K. Wang, K.R. Williams, W. Tan, An Autonomous and Controllable Light-Driven DNA Walking Device, Angewandte Chemie International Edition 51(10) (2012) 2457-2460.

[3] D. Wang, C. Vietz, T. Schroder, G. Acuna, B. Lalkens, P. Tinnefeld, A DNA Walker as a Fluorescence Signal Amplifier, Nano Lett 17(9) (2017) 5368-5374.

[4] J. Jiang, P. Zhang, Y.-m. Nie, K.-f. Peng, Y. Zhuo, Y.-q. Chai, R. Yuan, A well-directional three-dimensional DNA walking nanomachine that runs in an orderly manner, Chemical Science 11(8) (2020) 2193-2199.

[5] C. Jung, P.B. Allen, A.D. Ellington, A Simple, Cleated DNA Walker That Hangs on to Surfaces, ACS Nano 11(8) (2017) 8047-8054.

[6] M. Oishi, K. Saito, Simple Single-Legged DNA Walkers at Diffusion-Limited Nanointerfaces of Gold Nanoparticles Driven by a DNA Circuit Mechanism, ACS Nano 14(3) (2020) 3477-3489.

[7] L. Zhao, R. Sun, P. He, X. Zhang, Ultrasensitive Detection of Exosomes by Target-Triggered Three-Dimensional DNA Walking Machine and Exonuclease III-Assisted Electrochemical Ratiometric Biosensing, Anal Chem 91(22) (2019) 14773-14779.

[8] C. Jung, P.B. Allen, A.D. Ellington, A stochastic DNA walker that traverses a microparticle surface, Nature Nanotechnology 11(2) (2016) 157-163.

[9] K. Yang, H. Wang, N. Ma, M. Zeng, H. Luo, D. He, Programmable Target-Initiated DNAzyme Walker Walking along a Spatially Isolated and Highly Hybridizable Substrate Track on a Nanoparticle Surface, ACS Appl Mater Interfaces 10(51) (2018) 44546-44553.

[10] X. Qu, D. Zhu, G. Yao, S. Su, J. Chao, H. Liu, X. Zuo, L. Wang, J. Shi, L. Wang, W. Huang, H. Pei, C. Fan, An Exonuclease III-Powered, On-Particle Stochastic DNA Walker, Angew Chem Int Ed Engl 56(7) (2017) 1855-1858.

[11] Y. Wang, N. Hu, C. Liu, C. Nie, M. He, J. Zhang, Q. Yu, C. Zhao, T. Chen, X. Chu, An RNase H-powered DNA walking machine for sensitive detection of RNase H and the screening of related inhibitors, Nanoscale 12(3) (2020) 1673-1679.

[12] M. Hu, D. Mao, X. Liu, L. Ren, M. Zhou, X. Chen, X. Zhu, An all-in-one homogeneous DNA walking nanomachine and its application for intracellular analysis of miRNA, Theranostics 9(20) (2019) 5914-5923.

[13] N. Li, J. Zheng, C. Li, X. Wang, X. Ji, Z. He, An enzyme-free DNA walker that moves on the surface of functionalized magnetic microparticles and its biosensing analysis, Chemical Communications 53(60) (2017) 8486-8488.

[14] T. Chen, Y. Chen, H. Chen, F. Zhang, Q. Zhang, G. Chen, X. Zhu, Dual-enzyme-propelled unbounded DNA walking nanomachine for intracellular imaging of lowly expressed microRNA, Nano Research 12(5) (2019) 1055-1060.

[15] P. Yang, Y. Li, S.D. Mason, F. Chen, J. Chen, R. Zhou, J. Liu, X. Hou, F. Li, Concentric DNA Amplifier That Streamlines In-Solution Biorecognition and On-Particle Biocatalysis, Anal Chem 92(4) (2020) 3220-3227.

[16] X. Yang, Y. Tang, S.D. Mason, J. Chen, F. Li, Enzyme-Powered Three-Dimensional DNA Nanomachine for DNA Walking, Payload Release, and Biosensing, ACS Nano 10(2) (2016) 2324-2330.

[17] C. Yuan, J. Fang, Q. Duan, Q. Yan, J. Guo, T. Yuan, G. Yi, Two-layer three-dimensional DNA walker with highly integrated entropy-driven and enzyme-powered reactions for HIV detection, Biosens Bioelectron 133 (2019) 243-249.

[18] Y. Li, G.A. Wang, S.D. Mason, X. Yang, Z. Yu, Y. Tang, F. Li, Simulation-guided engineering of an enzyme-powered three dimensional DNA nanomachine for discriminating single nucleotide variants, Chem Sci 9(30) (2018) 6434-6439.

[19] E. Xiong, D. Zhen, L. Jiang, X. Zhou, Binding-Induced 3D-Bipedal DNA Walker for Cascade Signal Amplification Detection of Thrombin Combined with Catalytic Hairpin Assembly Strategy, Analytical Chemistry 91(23) (2019) 15317-15324.

[20] H. Chai, P. Miao, Bipedal DNA Walker Based Electrochemical Genosensing Strategy, Anal Chem 91(8) (2019) 4953-4957.

[21] A. Chen, Y. Zhuo, Y. Chai, R. Yuan, Bipedal DNA walker mediated enzyme-free exponential isothermal signal amplification for rapid detection of microRNA, Chemical Communications 55(92) (2019) 13932-13935.

[22] S.D. Mason, G.A. Wang, P. Yang, Y. Li, F. Li, Probing and Controlling Dynamic Interactions at Biomolecule-Nanoparticle Interfaces Using Stochastic DNA Walkers, ACS Nano 13(7) (2019) 8106-8113.

[23] R. Zhang, J. Zhang, X. Qu, S. Li, Y. Zhao, S. Liu, Y. Wang, J. Huang, J. Yu,

Efficient strand displacement amplification via stepwise movement of a bipedal DNA walker on an electrode surface for ultrasensitive detection of antibiotics, Analyst 145(8) (2020) 2975-2981.

[24] D. Kim, O.B. Garner, A. Ozcan, D. Di Carlo, Homogeneous Entropy-Driven Amplified Detection of Biomolecular Interactions, ACS Nano 10(8) (2016) 7467-7475.

[25] M. Ihira, T. Yoshikawa, Y. Enomoto, S. Akimoto, M. Ohashi, S. Suga, N. Nishimura, T. Ozaki, Y. Nishiyama, T. Notomi, Y. Ohta, Y. Asano, Rapid Diagnosis of Human Herpesvirus 6 Infection by a Novel DNA Amplification Method, Loop-Mediated Isothermal Amplification, Journal of Clinical Microbiology 42(1) (2004) 140.

[26] Y. Zhao, F. Chen, Q. Li, L. Wang, C. Fan, Isothermal Amplification of Nucleic Acids, Chemical Reviews 115(22) (2015) 12491-12545.

[27] Y. Xu, Y. Wang, S. Liu, J. Yu, H. Wang, Y. Guo, J. Huang, Ultrasensitive and rapid detection of miRNA with three-way junction structure-based trigger-assisted exponential enzymatic amplification, Biosens Bioelectron 81 (2016) 236-241.

[28] R. Li, Q. Liu, Y. Jin, B. Li, G-triplex/hemin DNAzyme: An ideal signal generator for isothermal exponential amplification reaction-based biosensing platform, Anal Chim Acta 1079 (2019) 139-145.

[29] Y. Sun, Y. Sun, W. Tian, C. Liu, K. Gao, Z. Li, A novel restriction endonuclease GlaI for rapid and highly sensitive detection of DNA methylation coupled with isothermal exponential amplification reaction, Chem Sci 9(5) (2018) 1344-1351.

[30] J. Chen, X. Zhou, Y. Ma, X. Lin, Z. Dai, X. Zou, Asymmetric exponential amplification reaction on a toehold/biotin featured template: an ultrasensitive and specific strategy for isothermal microRNAs analysis, Nucleic Acids Research 44(15) (2016) e130-e130.

[31] H. Jia, Z. Li, C. Liu, Y. Cheng, Ultrasensitive Detection of microRNAs by Exponential Isothermal Amplification, Angewandte Chemie International Edition 49(32) (2010) 5498-5501.

[32] M.S. Reid, X.C. Le, H. Zhang, Exponential Isothermal Amplification of Nucleic Acids and Assays for Proteins, Cells, Small Molecules, and Enzyme Activities: An EXPAR Example, Angew Chem Int Ed Engl 57(37) (2018) 11856-11866.

[33] R. Kumarswamy, I. Volkmann, T. Thum, Regulation and function of miRNA-21 in health and disease, RNA Biology 8(5) (2011) 706-713.

[34] G. Gines, R. Menezes, K. Nara, A.-S. Kirstetter, V. Taly, Y. Rondelez, Isothermal digital detection of microRNAs using background-free molecular circuit, Science Advances 6(4) (2020) eaay5952.

[35] X. Chen, K. Xu, J. Li, M. Yang, X. Li, Q. Chen, C. Lu, H. Yang, Switch-conversional ratiometric fluorescence biosensor for miRNA detection, Biosensors and Bioelectronics 155 (2020) 112104.

[36] J. Ge, Y. Hu, R. Deng, Z. Li, K. Zhang, M. Shi, D. Yang, R. Cai, W. Tan, Highly Sensitive MicroRNA Detection by Coupling Nicking-Enhanced Rolling Circle Amplification with MoS2 Quantum Dots, Analytical Chemistry 92(19) (2020) 13588-13594.

[37] T.J. Hellyer, J.G. Nadeau, Strand displacement amplification: a versatile tool for molecular diagnostics, Expert Review of Molecular Diagnostics 4(2) (2004) 251-261.

[38] R. Pieper, C.L. Gatlin, A.J. Makusky, P.S. Russo, C.R. Schatz, S.S. Miller, Q. Su, A.M. McGrath, M.A. Estock, P.P. Parmar, M. Zhao, S.T. Huang, J. Zhou, F. Wang, R. Esquer-Blasco, N.L. Anderson, J. Taylor, S. Steiner, The human serum proteome: display of nearly 3700 chromatographically separated protein spots on two-dimensional electrophoresis gels and identification of 325 distinct proteins, Proteomics 3(7) (2003) 1345-64.

[39] E. Hosseinzadeh, H. Ravan, A. Mohammadi, H. Pourghadamyari, Colorimetric detection of miRNA-21 by DNAzyme-coupled branched DNA constructs, Talanta 216 (2020) 120913.

[40] L. Yang, Q. Wu, Y. Chen, X. Liu, F. Wang, X. Zhou, Amplified MicroRNA Detection and Intracellular Imaging Based on an Autonomous and Catalytic Assembly of DNAzyme, ACS Sens 4(1) (2019) 110-117.

[41] Z. He, Y. Cai, Z. Yang, P. Li, H. Lei, W. Liu, Y. Liu, A dual-signal readout enzyme-free immunosensor based on hybridization chain reaction-assisted formation of copper nanoparticles for the detection of microcystin-LR, Biosens Bioelectron 126 (2019) 151-159.

[42] Y.-X. Cui, X.-N. Feng, Y.-X. Wang, H.-Y. Pan, H. Pan, D.-M. Kong, An integrated-molecular-beacon based multiple exponential strand displacement amplification strategy for ultrasensitive detection of DNA methyltransferase activity, Chemical Science 10(8) (2019) 2290-2297.

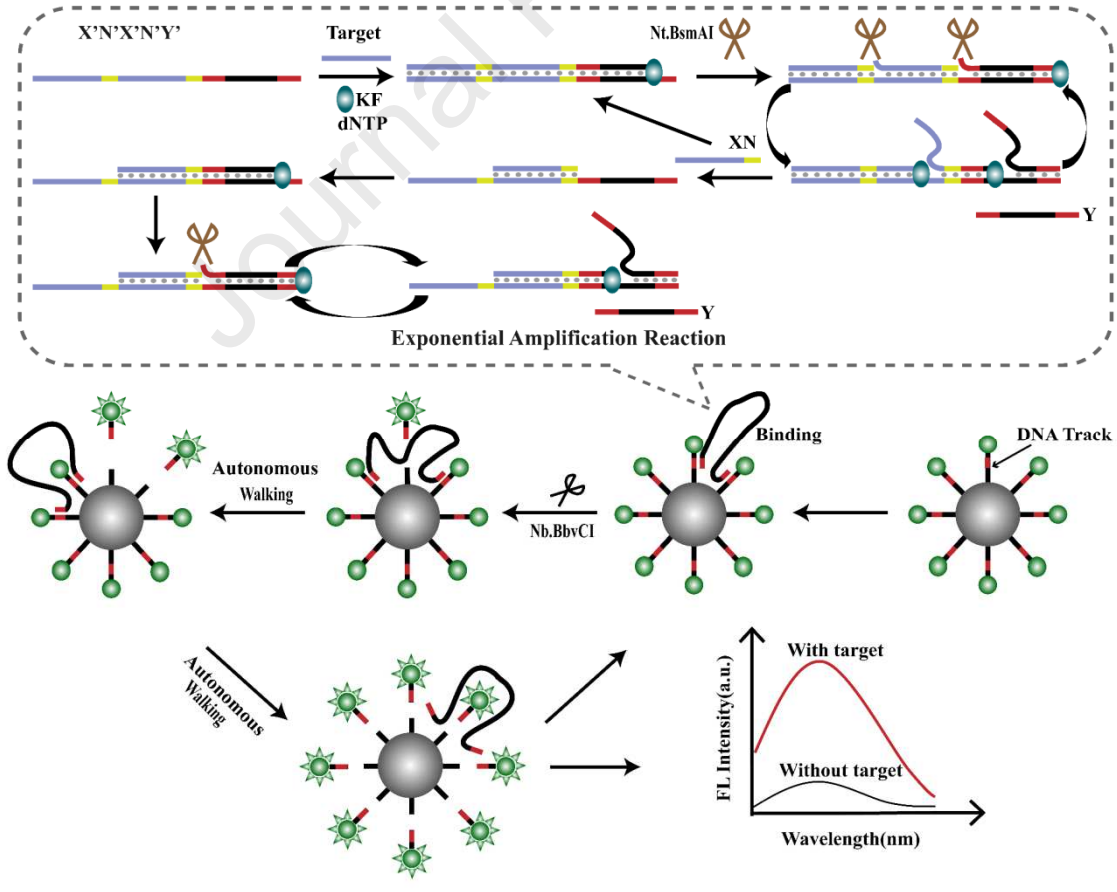

Scheme 1. Schematic illustration of EXPAR-BDW strategy based on exponential amplification reaction-triggered three-dimensional bipedal DNA walkers.

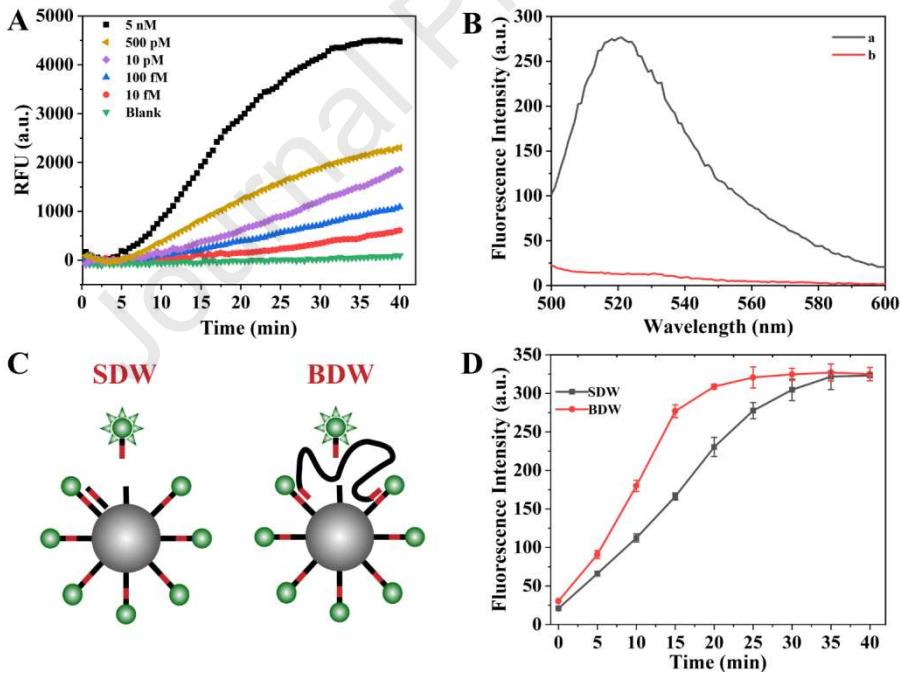

Fig. 1. (A) The time-dependent increase in fluorescence signals of EXPAR at different target concentrations. (B) The enzymatic cleavage reaction of BDW (a: with BDW, b: without BDW). (C) Schematic illustration the walking behavior using SDW and BDW. (D) The fluorescence signals of SDW and BDW at different assay times (0, 5, 10, 15,

20, 25, 30, 35 and 40 min). Error bars were obtained from triplex independent experiments.

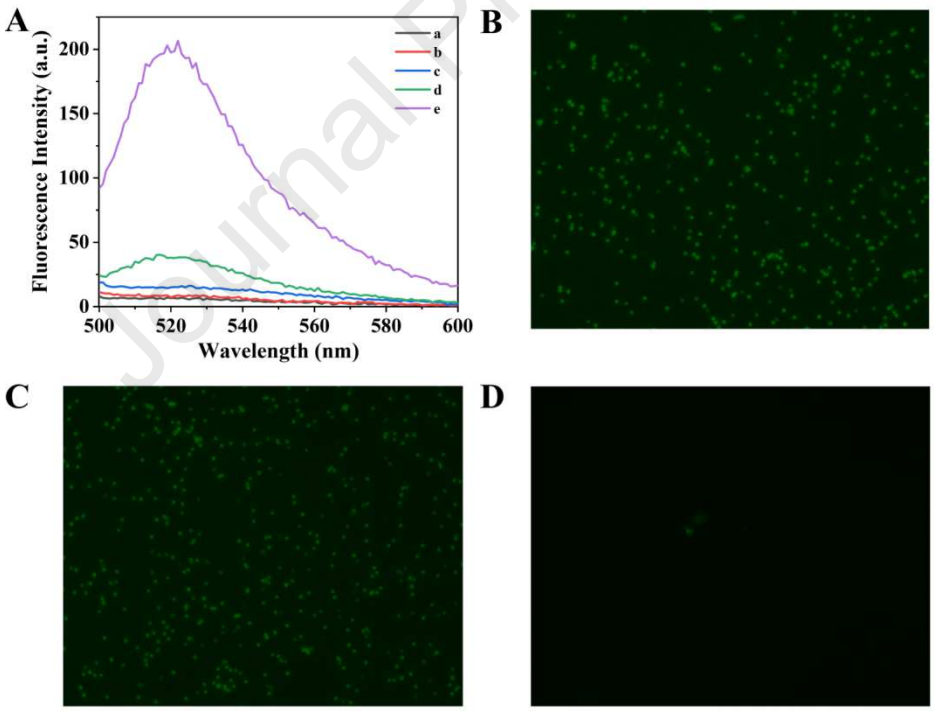

Fig. 2. (A) Fluorescence spectra of samples measured in different experimental conditions: (a) no KF polymerase; (b) no Nt.BsmAI; (c) no Nb.BbvCI; (d) no target; (e) with all experimental elements. Images of green microspheres acquired: (B) before

reaction; (C) after no target adding; (D) after target adding.

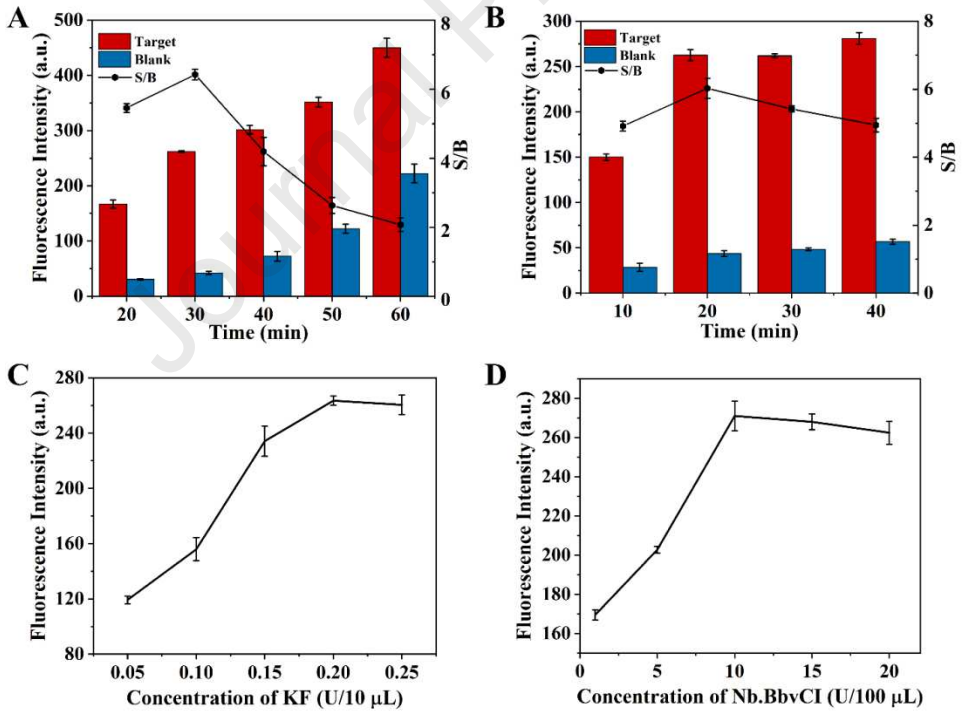

Fig. 3. (A) Fluorescence intensity and S/B ratio at different EXPAR reaction time. (B) Fluorescence intensity and S/B ratio at different BDW reaction time. (C) Fluorescence

intensity related to various concentrations of KF polymerase. (D) Fluorescence intensity related to various concentrations of Nb.BbvCI. Error bars were obtained from triplex independent experiments. S/B represents signal to background signal ratio.

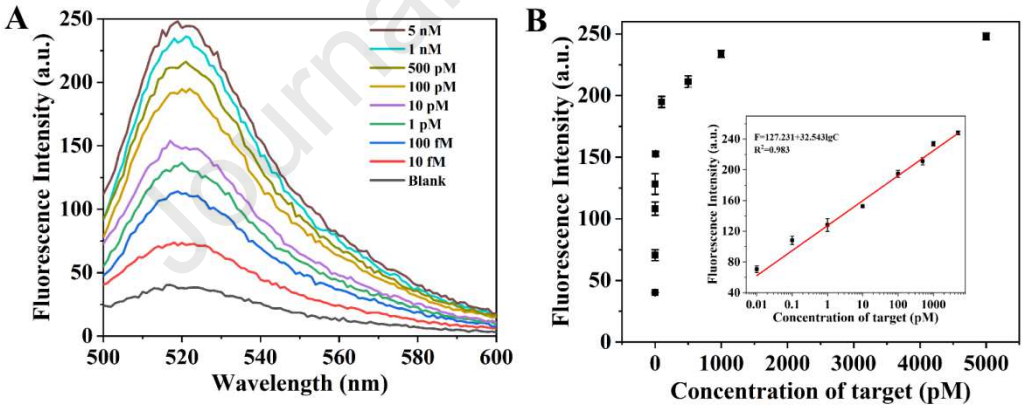

Fig. 4. Analytical performance of the biosensor. (A) Fluorescence emission spectrum at different target concentrations. (B) Linear correlation between the fluorescence intensity and target concentrations from 10 fM to 5 nM. Error bars were obtained from triplex independent experiments.

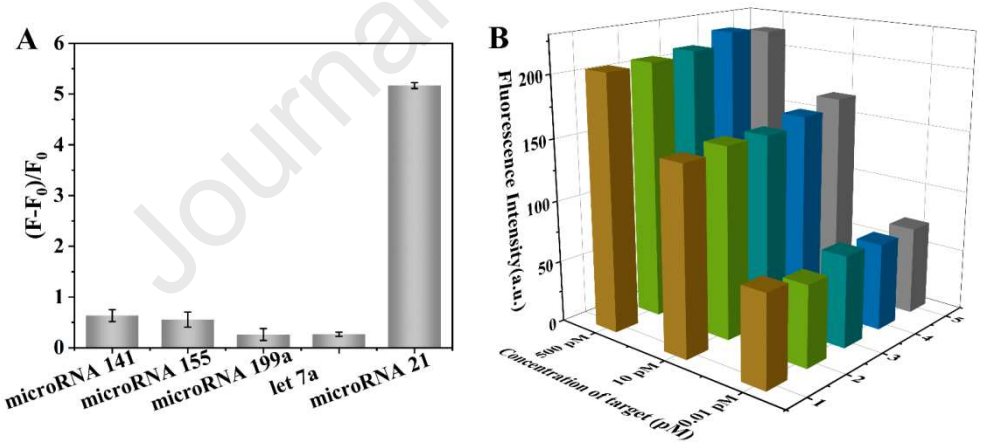

Fig. 5. (A) The selectivity of the biosensor towards different microRNAs. The concentrations of microRNAs were 5 nM. Error bars were obtained from triplex independent experiments. (B) Reproducibility of the biosensor at different concentrations for five independent experiments.

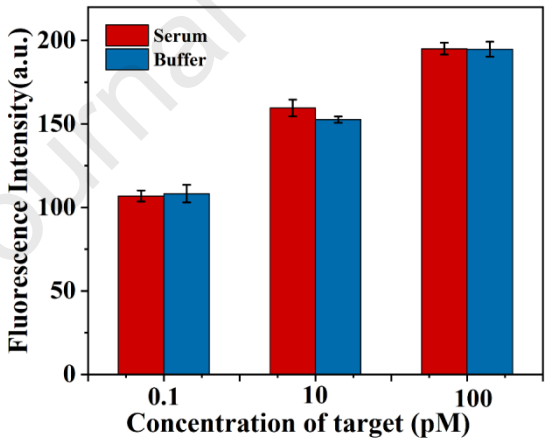

Fig. 6. Comparative data on the fluorescence signal obtained by different concentrations of microRNA 21 (0.1, 10, 100 pM) in buffer and diluted serum samples. Error bars were obtained from triplex independent experiments.

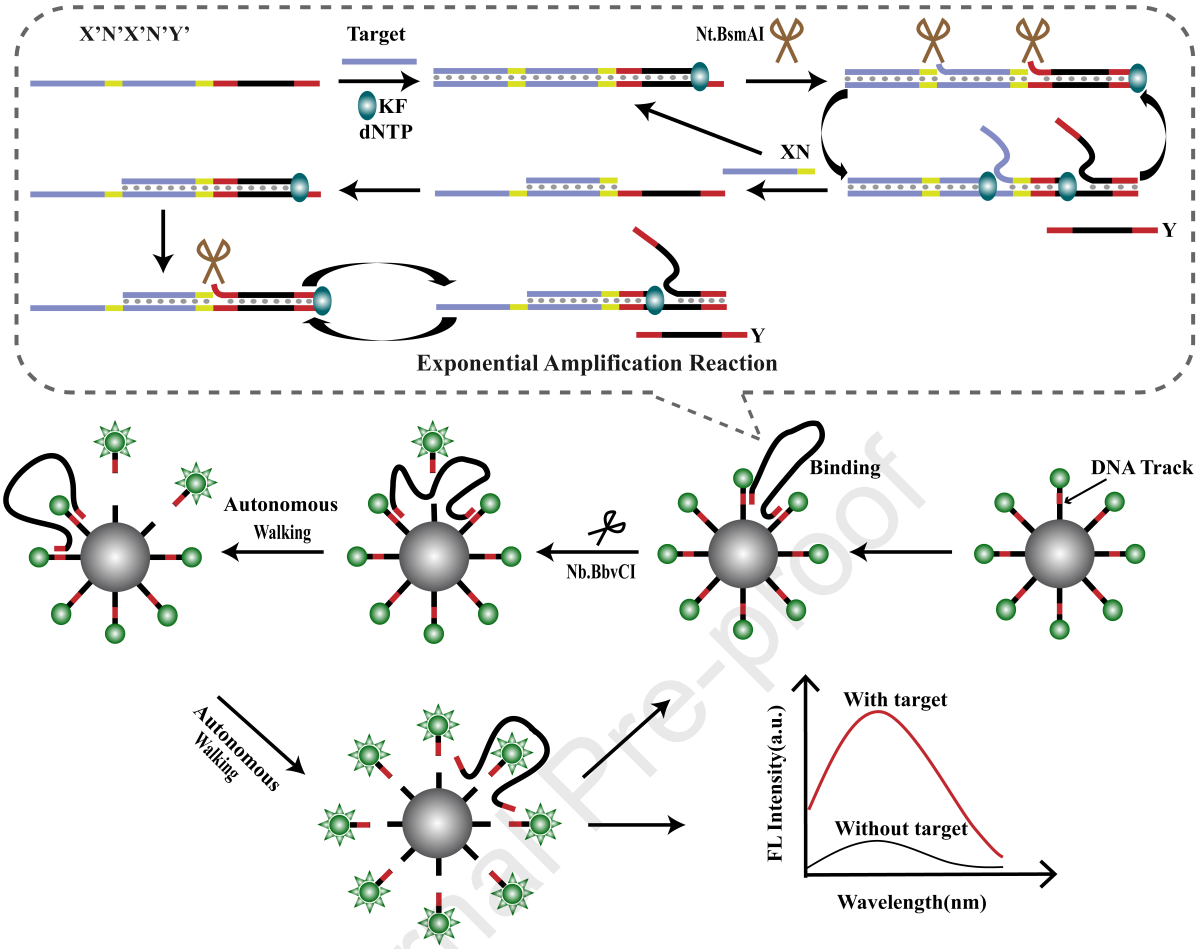

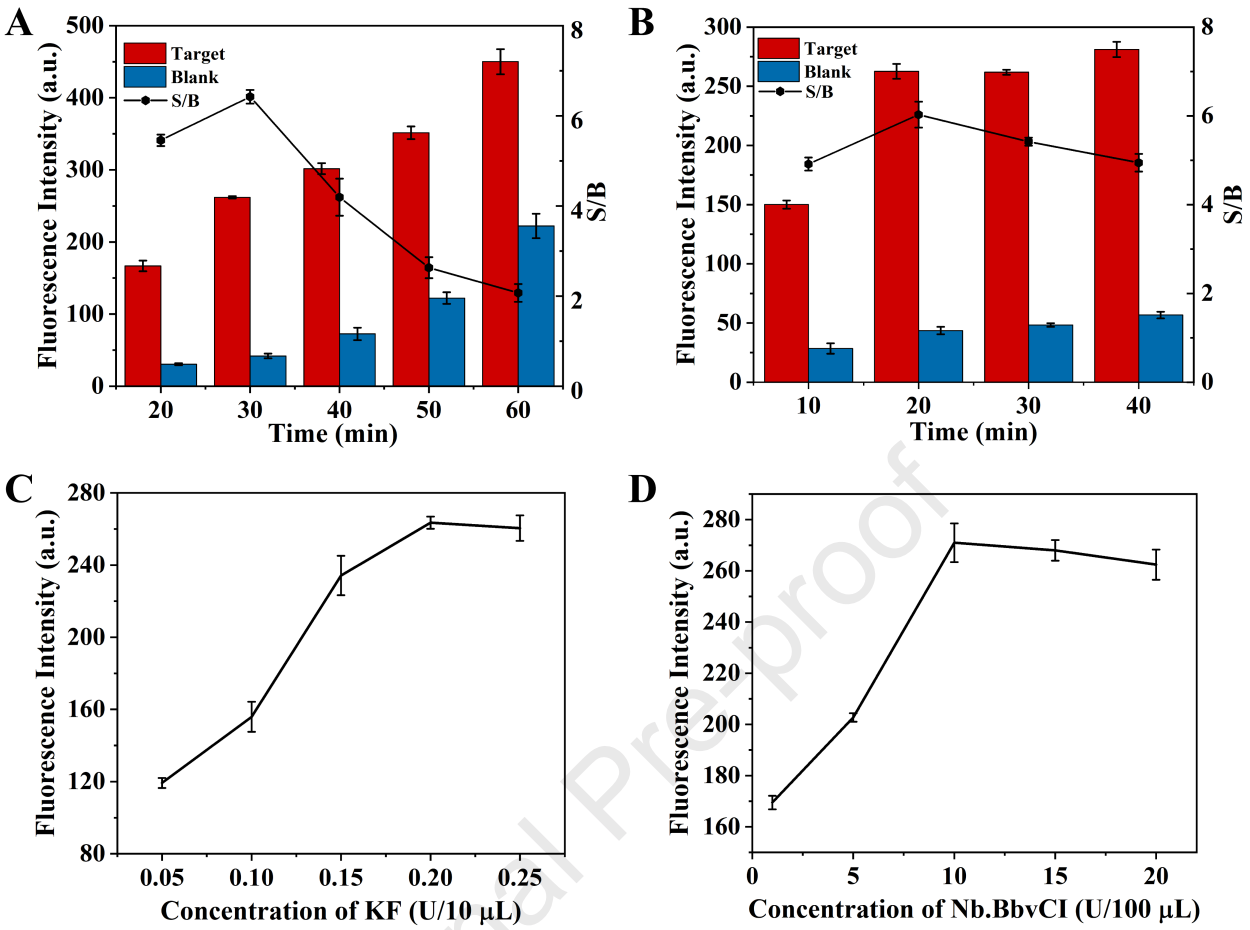

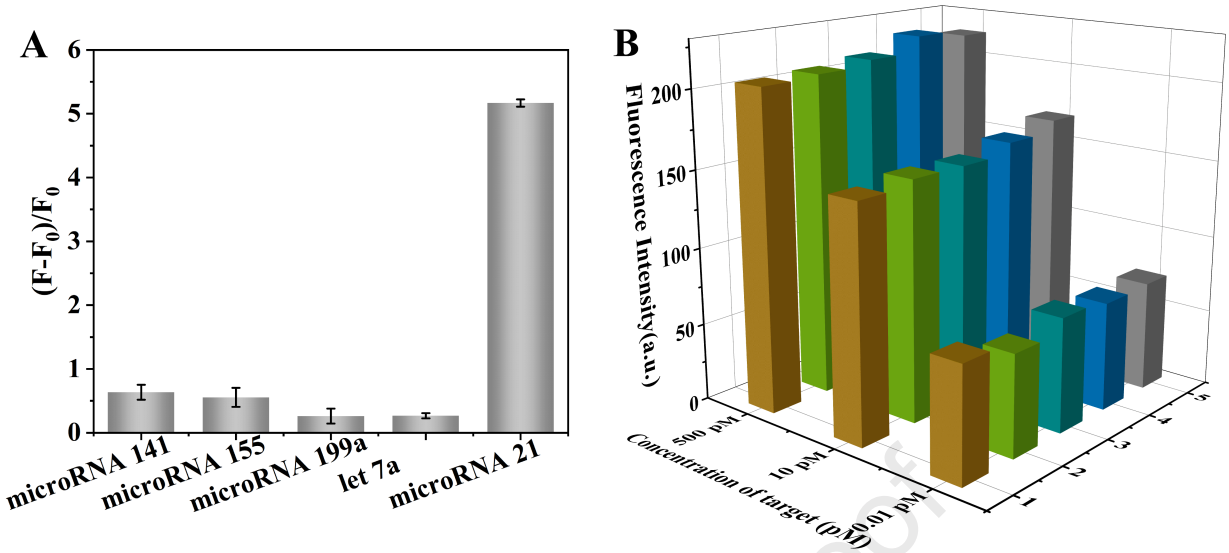

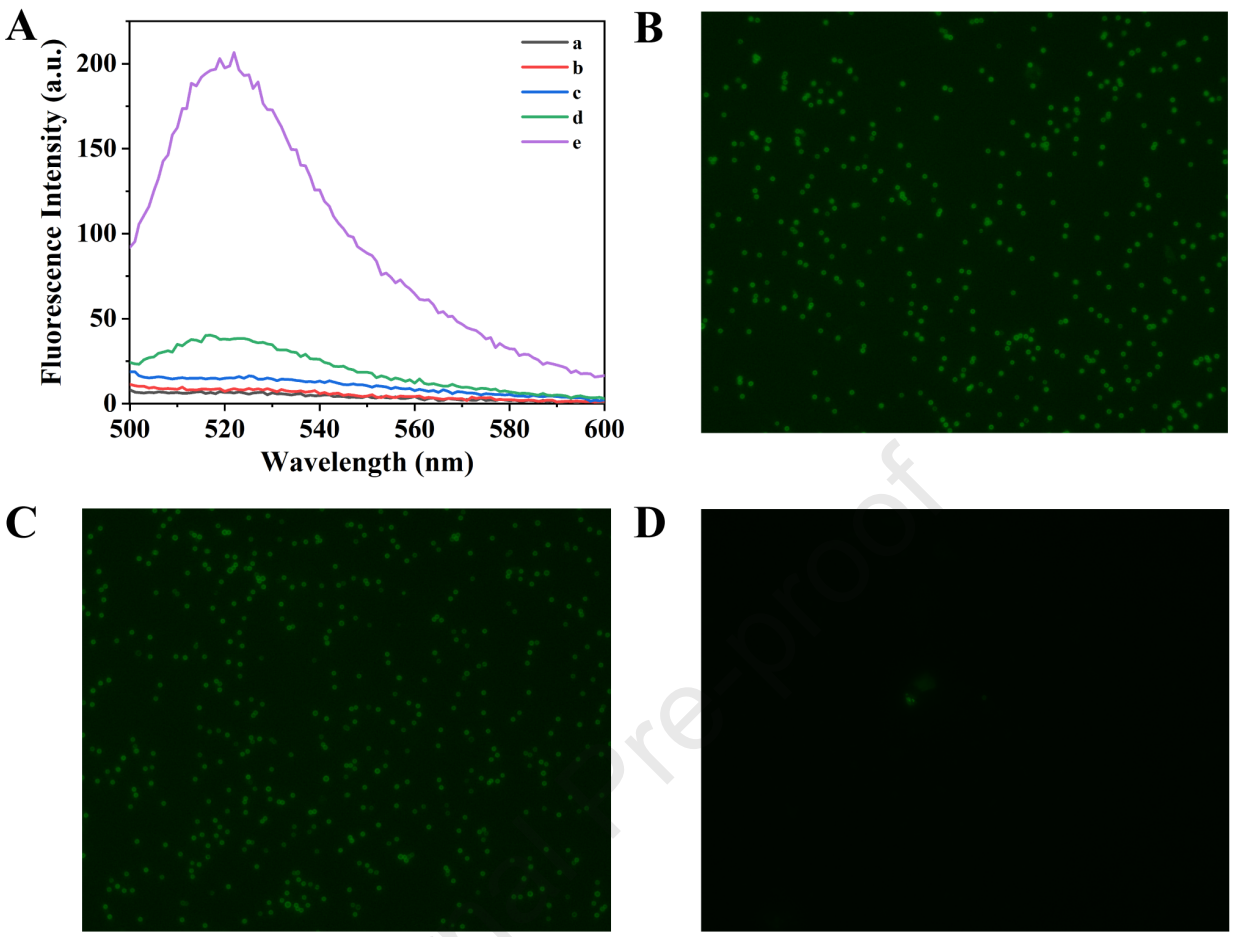

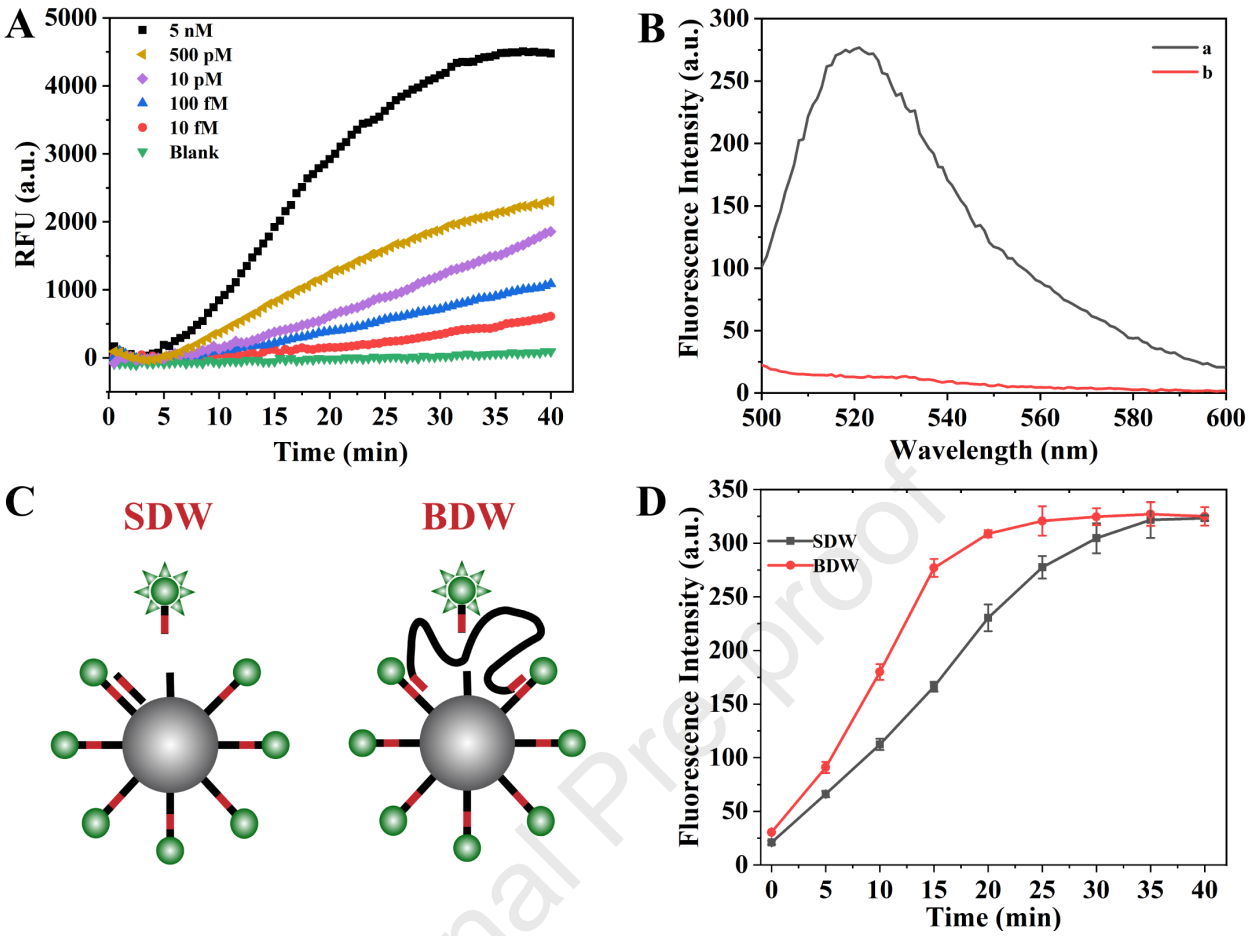

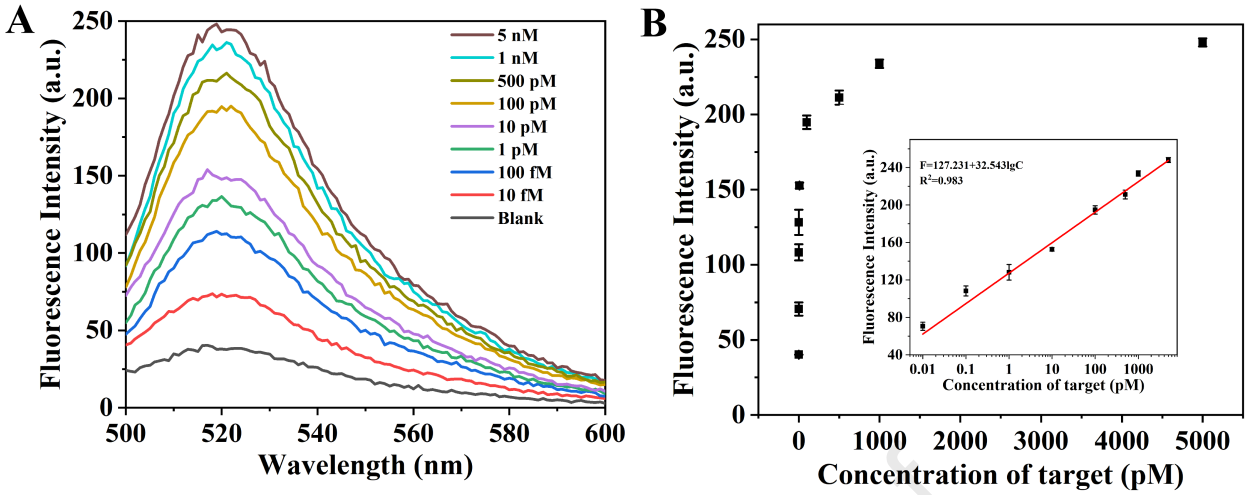

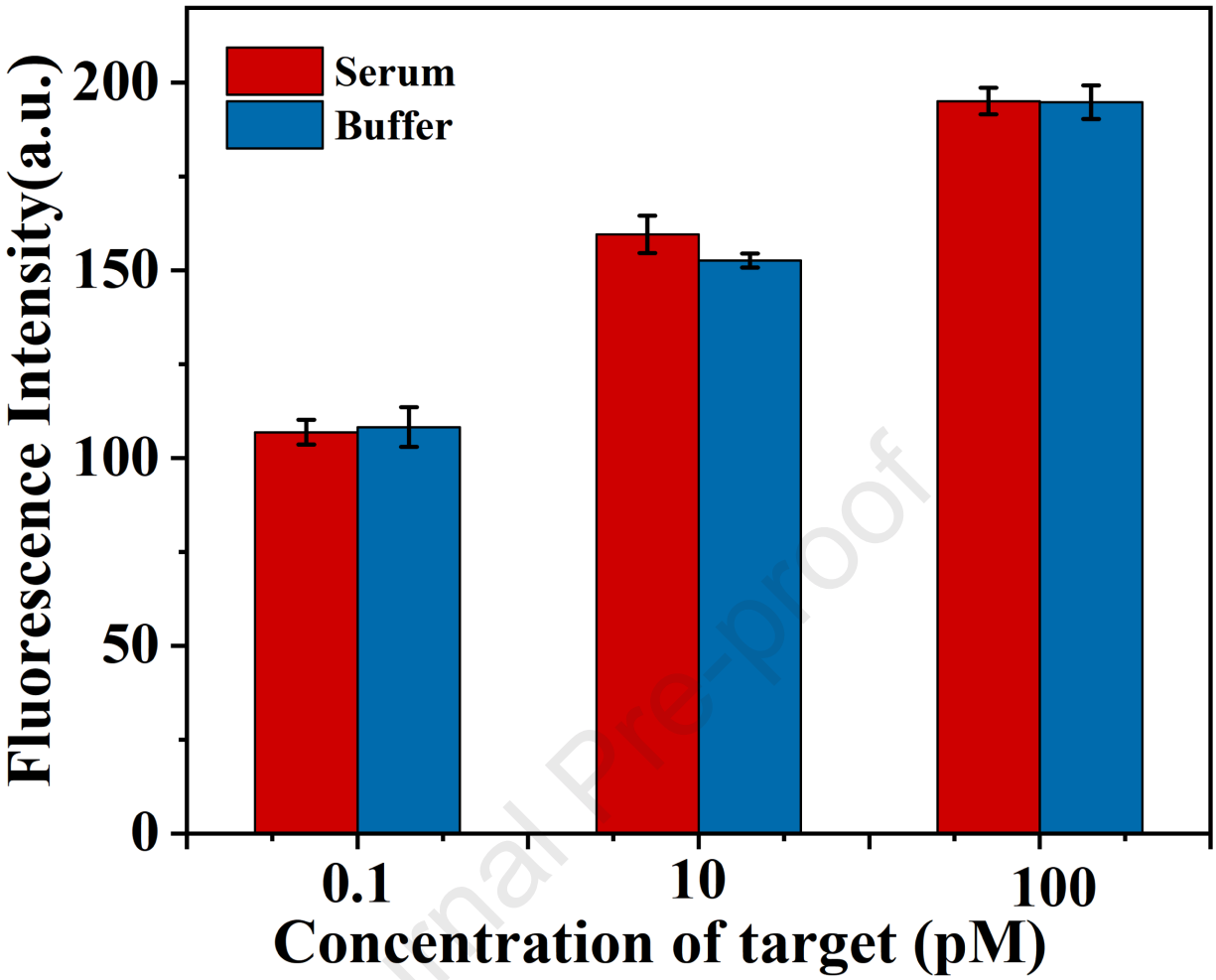

Highlights

1. A strategy for detection microRNA was constructed based on exponential amplification reaction and three-dimensional bipedal DNA walkers.

2. The proposed assay shows high sensitivity towards target microRNA 21 with a detection limit of 5.2 fM.

3. This method is simple in nucleic acid design and can be completed in short measurement time.

Declaration of interests

☒ The authors declare that they have no known competing financial interests or personal relationships that could have appeared to influence the work reported in this paper.

☐The authors declare the following financial interests/personal relationships which may be considered as potential competing interests: